Research Article
https://doi.org/10.1631/jzus.B2300275

Comparative study of bladder augmentation using PLLA-based biomimetic scaffolds: electrospun nanofiber vs. extracellular matrix scaffold with adipose-derived stem cells

Xuesheng WANG[1,2*], Dezhi ZHOU[3,4,5*], Liliang OUYANG[3,4,5], Fan ZHANG[1], Xu TAO[6]✉,Limin LIAO[1,2,7,8]✉

[1]*Department of Urology, China Rehabilitation Research Center, School of Rehabilitation of Capital Medical University, Beijing 100068, China*
[2]*University of Health and Rehabilitation Sciences, Qingdao, 266000, China.*
[3]*Department of Mechanical Engineering, Tsinghua University, Beijing 100084, China*
[4]*Biomanufacturing and Rapid Forming Technology Key Laboratory of Beijing, Tsinghua University, Beijing 100084, China*
[5]*"Biomanufacturing and Engineering Living Systems" Innovation International Talents Base (111 Base), Tsinghua University, Beijing 100084, China*
[6]*Center for Bio-intelligent Manufacturing and Living Matter Bioprinting, Research Institute of Tsinghua University in Shenzhen, Shenzhen, People's Republic of China*
[7]*China Rehabilitation Science Institute, Beijing, 100068, China*
[8]*Cheeloo College of Medicine, Shandong University, Jinan 250012, China.*

Unedited

Abstract: Bladder augmentation with gastrointestinal segments is a widely used surgical procedure for neurogenic bladder or bladder defects, but it carries a risk of many side effects, including metabolic disturbance, urolithiasis, and even malignancy. Several degradable materials have been used to investigate the regeneration of bladder tissue but few biomaterials have been translated into clinical applications. Moreover, there has been no systematic study of whether biomaterials applied in clinical practice are preferable for bladder tissue regeneration. The aim of this study was to compare the safety and applicability of small intestinal submucosa (SIS), poly(l-lactic) acid (PLLA) nanofibrous scaffold, and PLLA/gelatin composite nanofibrous scaffold as a potential bladder wall substitute material in tissue-engineered bladder augmentation and reconstruction. The results provide a scientific basis for selecting appropriate materials in clinical application. The microstructure, cytocompatibility, cell adhesion and histocompatibility of scaffolds, including SIS, PLLA nanofiber scaffold, and PLLA/gelatin were observed. Furthermore, bladder augmentation rabbit models were constructed using scaffolds with and without adipose-derived stem cell (ASC) implantation. All animals survived the experiment with no complications, and the structural integrity of the implantation site was demonstrated using cystography and urodynamics. Histological and immunohistochemical analyses indicated that the three kinds of scaffold could regenerate the bladder wall structure at 6 and 12 weeks. The animal models of ASC implantation confirmed their positive effect on urothelial maturation, smooth-muscle bundle and blood vessel regeneration, and physiological function restoration. Bladders reconstructed with the ASC-PLLA scaffold showed superior structural and functional properties, with no significant differences in the regenerated urothelium, smooth muscle, or vessels of the ASC-PLLA and control groups. PLLA-based nanofiber scaffolds with proper cell adhesion and growth can be an ideal support scaffold for achieving clinical applications for bladder reconstruction.

Key words: Bladder augmentation and reconstruction; Tissue engineering; Adipose-derived stem cells; Nanofiber scaffolds; Small intestinal submucosa

✉Limin LIAO, lmliao@126.com
✉Tao XU, xut@tsinghua-sz.org
Limin LIAO, https://orcid.org/0000-0002-7092-6576
Xu TAO, https://orcid.org/0000-0002-5783-6859
Xuesheng WANG, https://orcid.org/0000-0002-5612-6804
Dezhi ZHOU, https://orcid.org/0000-0002-6739-3510
Liliang OUYANG, https://orcid.org/0000-0003-4177-8698
Fan Zhang, http://orcid.org/0000-0002-2496-2824

Received Apr. 25, 2023; Revision accepted Oct. 8, 2023;
Crosschecked xxx. xx, 20xx; Published online xxx. xx, 20xx

© Zhejiang University Press 2023

1 Introduction

The primary function of the bladder is to provide an allantoic capsule and enable controlled urination. However, bladder dysfunction resulting from dysplasia, cancer, or neurological diseases can lower the quality of life and be life-threatening. Bladder reconstruction is considered a viable option for management of refractory lower urinary tract dysfunction resulting from progressive declines in bladder function (Chua et al., 2020). Currently, bladder reconstruction with autogenous or exogenous gastrointestinal segments is regarded as the standard surgical procedure for those diseases (Lam Van Ba et al., 2015). However, postoperative complications such as metabolic disturbance, infection, urolithiasis, and even malignancy (Ajalloueian et al., 2018) have plagued most patients. To avoid these complications, innovative tissue engineering (TE) has become an alternative to traditional surgical treatment. With the development of tissue engineering technology, diverse natural or synthetic materials with distinct properties, with or without seeded cells and/or biological factors, have been used for bladder tissue regeneration (Wang et al., 2021).

Bladder substitutes derived from porcine small intestinal submucosa (SIS) or bladder acellular matrix (BAM), are typically made of extracellular matrix (ECM) via a process that removes cells and other immunogenic components (Deng et al., 2017). These substitutes are rich in many components, including collagen, proteoglycans, and functional growth factors, and facilitate the proliferation and differentiation of cells (Zhang et al., 2005; Pokrywczynska et al., 2021). However, their clinical application can lead to the formation of calculi due to their poor degradation rate (Zhang et al., 2006), bladder rupture caused by low mechanical strength (Zhang et al., 2006), and immunological problems leading to fibrosis (Zhang and Liao, 2020). In addition, the therapeutic effect of native-derived substitutes may require more effort to guarantee the homogeneity of products before full clinical application. On the other hand, absorbable synthetic material is an alternative due to its malleable properties, stable repeatability, good processability, and their ability to be easily tailored into required shapes and sizes. Poly(l-lactic) acid (PLLA) has been widely used in different areas of biomedicine by virtue of its advantageous mechanical, thermoplastic, biocompatible, and biodegradable properties (Derakhshan et al., 2016). Previous studies have confirmed that PLLA is a promising material for use in bladder tissue engineering (Tian et al., 2010; Derakhshan et al., 2016). In addition, a composite and biomimetic, nonwoven fiber scaffold composed of PLLA and gelatin also has proven suitable for repairing dura tissue defects, with optimal clinical effects (Deng et al., 2016; Deng et al., 2017).

Stem cells have high self-renewal and multidirectional differentiation capabilities and play an essential role in tissue regeneration (Pokrywczynska et al., 2018). In tissue engineering and regenerative medicine, autologous adipose-derived stem cells (ASCs) are now relatively abundant, readily harvested, and offer multipotential differentiation.

Biodegradable materials derived from a natural or synthetic matrix, generally defined as “bioprosthetic meshes”, are widely used in clinical surgical practice (Zhang and Liao, 2014; Shi et al., 2016). However, no systematic studies or reviews have been conducted to determine which biomaterials work best in tissue-engineered bladder augmentation and reconstruction. Hence, the purpose of our study was to investigate the safety and applicability of SIS, PLLA and PLLA/gelatin biomimetic materials, which are typical representatives of a natural acellular matrix, synthetic polymer materials, and composite materials, in tissue-engineered bladder augmentation. The findings from our study provide scientific evidence for selecting an appropriate material for clinical application and in-situ 3D bioprinting of bladder tissue. The safety and effectiveness of different materials were systematically evaluated via in vitro and in vivo experiments. The biological properties of these scaffolds including their cytotoxicity, cell adhesion and distribution, proliferation, and stemness maintenance, were compared in detail. We also investigated the performance of a reconstructed bladder using urodynamics, and compared the histological differences in tissue repair sites in an animal model. Furthermore, we evaluated the efficacy of scaffolds, with or without seed cells, to guide tissue regeneration.

Unedited

2 Materials and methods

2.1 Materials

Both the PLLA nanofiber scaffold (ReDura™) and PLLA /gelatin nanofiber scaffold (NeoduraTM), manufactured by electrospinning technology, were provided by Medprin Biotech GmbH (Frankfurt am Main, Germany). The fibrous structure of these materials is similar to the ECM of human organ tissues (Deng et al., 2016; Deng et al., 2017). The substitute used in this study was SIS from Cook Biotech (West Lafayette, IN, USA), which is fabricated with four layers of porous fibrillar collagen type I.

2.2 Cell cultures

Rabbit ASCs (Procell Life Science & Technology Co. Ltd., China) were cultured in rabbit ASC culture medium (Cyagen Biosciences, China) with 10% fetal bovine serum (FBS, Gibco). The culture medium containing cells was incubated in a humidified chamber (5% carbon dioxide) at 37◦ C, with medium changes every 2 or 3 days. ASCs were harvested when cells reached 80 to 85% confluence, and passages three and four were used for the experiments. The species of ASCs applied in in vivo experiments was determined by the experimental animal species to reduce the possibility of immunological rejection.

2.3 Scaffold treatment

Before seeding cells, the scaffolds were immersed in PBS solution and placed on a shaker (70 rpm) at 37° C for 24 h. To evaluate internal cell adhesion, scaffolds immersed in PBS with 1 μg/cm2 fibronectin (Sciencell, USA) were used as positive controls. First, the fibronectin (FBN) was diluted with PBS solution to acquire the desired coating solution. Second, after placing the PLLA and PLLA/gelatin scaffolds (1.5×1.5 cm) into 24-well plates, 1 mL of coating solution was added to each well to prepare the FBN-coated scaffold. After 24 h, all scaffolds were washed with PBS twice and placed on a new 24-well plate for cell seeding. Several studies have proven the feasibility of SIS as an alternative implantation for bladder reconstruction (Wang and Liao, 2014; Zhang and Liao, 2014). An untreated SIS scaffold was chosen for comparison in this work. Therefore, the cytotoxicity and adhesiveness of SIS were not evaluated in this study.

2.4 Cell seeding and attachment

First, the optimal seeding density was determined according to the attachment rate of different cell densities on PLLA and PLLA/gelatin scaffolds. After cell harvesting and counting, the ASCs were resuspended in culture medium, and 1 mL of cell suspension (0.1×106/mL, 0.15×106/mL, 0.3×106/mL, 0.4×106/mL) was added to the scaffold wells. The scaffolds were then placed in an incubator for culture. After 12 h, to eliminate the effect of unattached cells in the plate, all scaffolds were washed with PBS twice and placed in a new 12-well plate to determine the optimal cell density. Second, to investigate the cell adhesion property of the scaffolds, equal seeding densities of ASCs (0.15 × 106 cells/mL) were added to coated and uncoated scaffolds as well as the culture dish. A Cell Counting Kit-8 (Yeasen, China) was used to estimate the cell number based on the supernatant’s optical density (OD), which was read using a microplate reader (Thermo Fisher, USA) at a wavelength of 450 nm. The scaffold's cell attachment was measured as the ratio of the OD of the scaffold to the OD of the culture dish. We also seeded cells onto scaffolds at a density of 0.15 × 106 cells/mL to evaluate the effect of the coating on cell proliferation by measuring the OD on days 2, 5, 7 and 14. The OD values of each group were normalized to day 1 for plotting and statistics.

2.5 Flow cytometry analysis

The phenotype maintenance of ASCs cultured on the scaffold after 14 days was analyzed by flow cytometry. The monoclonal antibodies CD73-PE, CD90-PE, and CD105-PE (all from Thermo Fisher, USA) were used for analyses. The cells attached to the scaffold were easily harvested by digesting them with 0.25% (weight per volume) trypsin for 3 to 5 min. After centrifugation, cells were resuspended in PBS with monoclonal antibodies and incubated in the dark at room temperature for 20 min. Next, cells were washed and resuspended for testing. Control samples without staining were included to confirm specificity and for compensation settings. At least 10,000 events were acquired on the flow cytometer (NoVocyte, Agilent, USA) AIQ. Data were analyzed using Novoexpress.

Unedited

2.6 Cell proliferation and morphology

ASCs were seeded on each scaffold at a density of 0.15 × 106 cells/ mL per scaffold, and then the ASC-laden scaffolds were cultured in vitro for 1, 3 and 5 days to evaluate the cell morphology and cell adhesion area. FITC-phalloidin and DAPI (Yeasen, China) were used to mark the cytoskeleton and nucleus of ASCs after fixing the cell-laden scaffolds overnight at 4 ℃ with 4% paraformaldehyde (Leagene, China).

2.7 Scanning electron microscopy (SEM)

Microstructural analysis of the scaffolds was performed using a scanning electron microscope (SEM) (Gemini300, Zeiss, Germany). In addition, the morphology of the ASCs seeded on the scaffolds was investigated after 1, 3, and 5 days of culture to assess cell proliferation and distribution. The cell-laden scaffolds were fixed overnight at 4 ℃ in a mixture of 2% paraformaldehyde and 2.5% glutaraldehyde (Leagene, China), and dehydrated by soaking the samples in an ethanol gradient (70, 80, 90, 95, and 100%) for 10 min. Then the samples were freeze-dried and sprayed with gold before being photographed.

2.8 Histocompatibility

The histocompatibility and degradation of the tested materials in vivo were evaluated using subcutaneous implantation. An incision was made on the back, and ASC-free scaffolds and ASC-laden scaffolds (1×1 cm) were implanted subcutaneously. Then the implants and adjoining tissues were collected for histological evaluation after 6 weeks.

2.9 Bladder augmentation model

All procedures were approved by the Capital Medical University Laboratory Animal Welfare and Ethical Committee (NO: AEEI-2021-168). To construct the bladder augmentation model with an ASC-free scaffold, 35 male New Zealand rabbits (2.0 ± 0.3 kg) were divided into four groups: a sham group (n = 5); SIS group (n=10); PLLA group (n=10); and PLLA/gelatin group (n=10). Animals in each group were sacrificed 6 or 12 weeks after implantation (n = 5 rabbits per time point). ASCs were seeded at 0.15 × 106 cells/mL and cultured for 3-5 days for the in vivo experiments. To construct the bladder augmentation model with an ASC-laden scaffold, 15 male rabbits were divided into 3 groups: an ASC-SIS group (n=5); ASC-PLLA group (n=5); and ASC-PLLA/gelatin group (n=5). Briefly, all rabbits were anesthetized with a marginal ear vein injection of α-chloralose (80 mg/kg). A urodynamic assessment of each rabbit was made before surgery, then a median incision of the lower abdomen was made to expose the intact bladder. A longitudinal full-thickness incision (6 cm) was made in the anterior bladder wall, which was removed with silk marking stitches to create a 3×3-cm defect. Sterilized SIS, PLLA, and PLLA/gelatin scaffolds, with or without ASCs (2 ml, 0.15 million/mL), were sutured to the defect with degradable sutures (5-0 Monocryl, Johnson & Johnson, USA). Perivesical fat was secured over the graft, and the abdomen was closed layer by layer. Penicillin (400,000 U by muscle injection, Harbin Pharmaceutical Group Holding Co.) was administered daily for 3 days. All rabbits were housed individually and were sacrificed 12 weeks after implantation.

2.10 Cystography and Urodynamic examination

Cystographic and urodynamic tests were performed on all rabbits after implantation. Under α-chloralose anesthesia, a 3-F double-lumen catheter was inserted into the bladder. Cystography was performed with 30% iopamidol (Aladdin, China) infused into the bladder until stress incontinence occurred. X-rays were obtained from each bladder, and then one tube of the catheter was attached to a urodynamic system (MP 150, Biopac, CA, USA) to monitor the intravesical pressure (Pves), and the other lumen was connected to a perfusion pump to infuse (6 ml/min) the bladder with warm saline. When the first leakage was detected, the Pves and maximum bladder capacity (MBC) were recorded, and bladder compliance (BC) was calculated according to the equation $\Delta V/\Delta P$.

2.11 Histological and immunofluorescence (IF) assessment

After cystography and urodynamic analyses, the rabbits were sacrificed, and the whole bladder was obtained immediately. Bladder tissue samples were rinsed with cold saline and observed macroscopically. A full-thickness sample from the transplanted site was fixed with 10% formalin, dehydrated in an alcohol gradient, embedded in paraffin, and sectioned at 3~5 μm for hematoxylin and eosin (H&E) staining and Masson's

Unedited

trichrome staining (MTS). Bladder regeneration was evaluated using IF analysis with different antibodies against the urothelium (AE1/AE3, Abcam, ab9377), smooth muscle (a-SMA, Proteintech, 14395-1-AP), and vascular endothelium (CD31, Abcam, ab199012), and all sections were incubated with the secondary antibodies and DAPI. The area of positive staining and the number of vessels were quantified using Image-Pro Plus 6.0 software (Media Cybernetics, MD) in 10 different fields per sample.

2.12 Statistical analysis

All data are presented as mean ± SD. Statistical analysis was performed using GraphPad Prism v7.0 software. Differences between groups were analyzed using Student's t-test or analysis of variance (ANOVA). $P<0.05$ was considered significant.

3 Results

3.1 Cytocompatibility of scaffold

To determine the proper cell seeding density, we conducted cell seeding with different density suspensions. The results showed that the cell attachment ratio waned rapidly in the ASC-laden scaffold with a seeding density of 0.4 × 106 cells/ mL, and the 0.15-million-cell group had the highest cell attachment ratio (Figure 1A; excess cell density lowers the cell attachment). Further, we detected the cell attachment properties of the scaffolds by comparing the FBN-coated and FBN-uncoated scaffolds. There was no appreciable difference in cell attachment ratio between FBN-coated scaffolds and uncoated scaffolds at concentrations of 0.1 × 106 and 0.15 × 106 cells/ mL ASCs (Figure 1B). In addition, long-term culture of cells on FBN-coated and FBN-uncoated scaffolds were used to assess the effect of coating on proliferation of ASCs (0.15 million/mL). There were no obvious differences in cell proliferation between the FBN-uncoated group and the FBN-coated group, and cell numbers from all groups had significantly expanded (Figure 1C). After 14 days of culture, ASCs from all groups had maintained high expression of CD73, CD90, and CD105 (Figure 1D). These results demonstrate that both PLLA and PLLA/gelatin perform well in ASC attachment and proliferation, and support the feasibility of these scaffolds as cell-laden implantations for regeneration.

Unedited

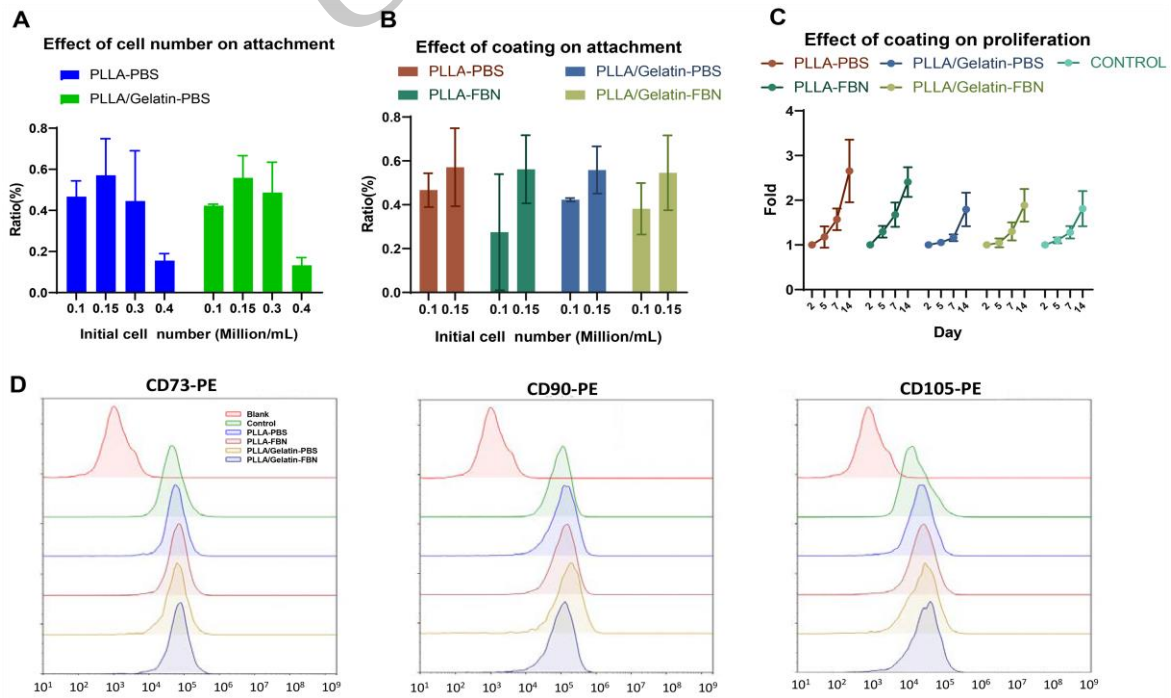

Fig. 1 Cytocompatibility of scaffold. (A) Effect of cell number on cell attachment in uncoated scaffolds; ratio = scaffold optical density value/culture dish optical density value. (B) Effect of fibronectin (FBN)-coating on cell attachment; ratio = scaffold optical density value/culture dish optical density value. (C) 0.15 million/mL cells seeded on both uncoated and fibronectin-coated scaffolds to study cell proliferation on day 14 of culture. (D) Key phenotype maintenance of adipose stem cells cultured on scaffolds for 14 days.

3.2 Distribution of cell-laden scaffold

SEM images revealed that the surface of the PLLA and PLLA/gelatin scaffolds appeared as nonwoven webs with open, interconnected pores to construct a unique 3D structure with nanofibers (Figure 2A). In contrast, the morphological characteristics of SIS scaffold were obviously different from those of the other two electrospun scaffolds. The surface of the SIS scaffold was flat and smooth and without pores (Figure 2A). The ASC-laden scaffolds were cultured in vitro, and the normal proliferation of ASCs in scaffolds was observed at days 1, 3 and 5 using SEM. Furthermore, cell morphology and adhesion area were captured during in vitro culture (Figure 2B-D). The figures indicate that most ASCs showed polygon-shape morphology and adhered to the surface of the PLLA, PLLA/gelatin nanofiber scaffolds, filling the pore spaces and forming a cell-coated bio-surface. However, cells attached to the SIS scaffold were spindle-shaped, with long processes. When ASCs were seeded on the three kinds of scaffolds at a density of 0.15 × 106 cells/mL, cells in the PLLA and PLLA/gelatin groups spread faster than those in the SIS group. This phenomenon demonstrates that PLLA and PLLA/gelatin can facilitate initial cell attachment. Further, we quantified the cell growth area to compare the cell proliferation on the three scaffolds (Figure 2E). There was no significant difference between the PLLA and PLLA/gelatin groups, and ASCs in all groups were distributed uniformly on the surface of the scaffold at day 5. However, the cell fluorescence area of SIS was significantly lower than those of the PLLA and PLLA/gelatin scaffolds on days 3 and 5. Combined with the cell proliferation and ASC flow cytometry results in Fig. 1, our results showed that both the PLLA and PLLA/gelatin scaffolds can support ASC culture without the FBN coating. Therefore, the pure, uncoated scaffolds and a cell density of 0.15 million/mL were used in the in vivo experiment.

Unedited

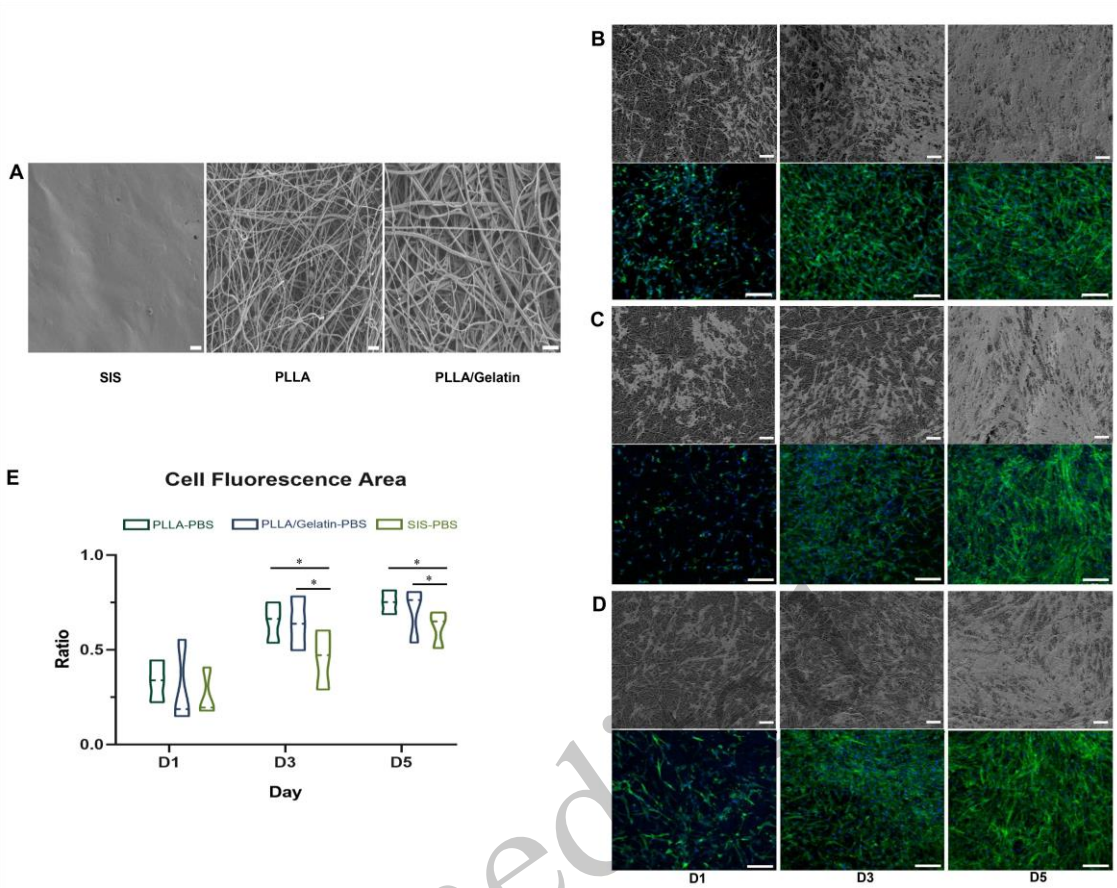

Fig. 2 Structural properties and cell distribution on scaffolds. (A) SEM micrographs of the SIS, PLLA, and PLLA/gelatin scaffolds. Scale bars = 10 μm. (B-D). Distribution of adipose stem cells on scaffolds in scanning electron microscopy, and cytoskeleton (green) and nucleus (blue) of ASCs attached on scaffold surface. Scale bars = 100 μm. (E) Semiquantitative evaluation of cell spreading area based on fluorescence images.

Unedited

3.3 Histocompatibility

Six weeks after subcutaneous SIS, PLLA, and PLLA/gelatin scaffold implantation, histological staining showed the scaffolds attracted infiltration of inflammatory cells at their periphery, but the three kinds of scaffolds showed different degrees of degradation. Collagen fibers were deposited in the degradation sites of the SIS scaffold, while a large number of inflammatory cells were observed around the PLLA and PLLA/gelatin scaffold. In contrast, the three kinds of ASC-laden scaffold showed a certain degree of degradation 6 weeks after subcutaneous implantation, and no obvious inflammatory reaction was observed from the histological evaluation. A rich infiltrate of cells was observed in three ASC-laden scaffolds (Supplementary Figure S1).

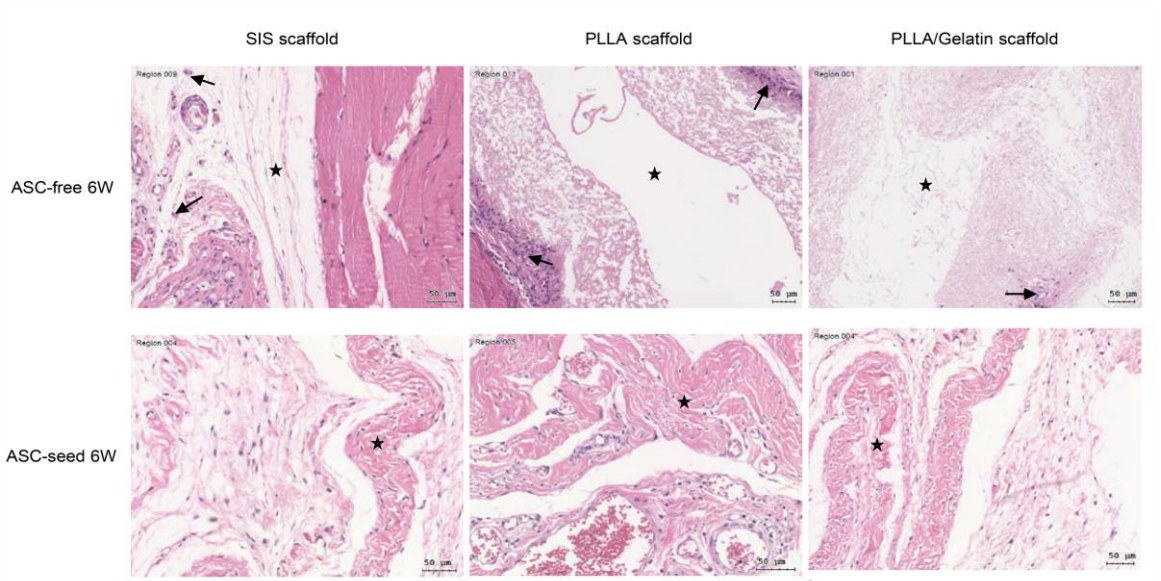

Supplementary Figure S1 Histologic evaluation of subdermally implanted scaffolds. →Indicates inflammatory cells, ★Indicates scaffolds. Scale bar = 50 μm.

Unedited

3.4 Cystography and urodynamic evaluation

All models underwent retrograde cystography at 6 and 12 weeks (Figure 3A), which confirmed that there was no leakage from the bladder in each group at 6 weeks. The bladder capacity of the experimental animal models fitted with the three scaffolds was reduced compared with that of the sham group. In addition, bladder calculi were found in the SIS, PLLA, and PLLA/gelatin groups at 6 weeks, and the incidence of bladder calculi in the three models was 40%, 20%, and 20%, respectively. A larger bladder with an extended, uneven profile was observed in the ASC-free scaffold groups at 12 weeks. Even though the bladder capacity of the ASC-free scaffold groups at 12 weeks enlarged markedly compared with those of the model groups at 6 weeks, an uneven profile of the reconstructed bladder was observed in those groups. Reconstructed bladders in ASC-laden scaffolds exhibited improved capacity and regular shape at 12 weeks, but the bladder body did not fully bulge to form a smooth configuration.

The physiological function of the repaired bladder was evaluated using urodynamic tests performed at 6 and 12 weeks after implantation. In the three kinds of ASC-free groups, there were no statistically significant differences in MBC at 6 weeks compared with the sham group (all $P>0.05$). The compliance of the regenerated bladder tissue in the three models was lower than that of the sham group ($P<0.05$) (Figure 3B, E). However, MBC increased 12 weeks after reconstruction using ASC-free SIS and PLLA nanofiber scaffolds compared with the sham group (68.04 ± 5.34 ml and 77.53 ± 8.87 ml vs. 58.88 ± 4.13 ml, $P<0.05$, respectively). The compliance of the reconstructed bladder in the ASC-free SIS and PLLA groups was similar to that of the native bladder (Figure 3C, F). Moreover, the MBC in the ASC-PLLA group at 12 weeks was significantly higher than that in the other groups (88.97 ±5.92 ml vs. 58.88 ± 4.13 ml, 75.17 ± 9.13 ml and 61.18± 8.40 ml, $P<0.05$, respectively). The compliance of the repaired bladder was similar to that of the native bladder (Figure 3D, H). However, no significant difference was observed in bladder capacity between the ASC-PLLA/gelatin group and the sham group (61.18± 8.40 ml vs. 58.88 ± 4.13 ml, $P>0.05$).

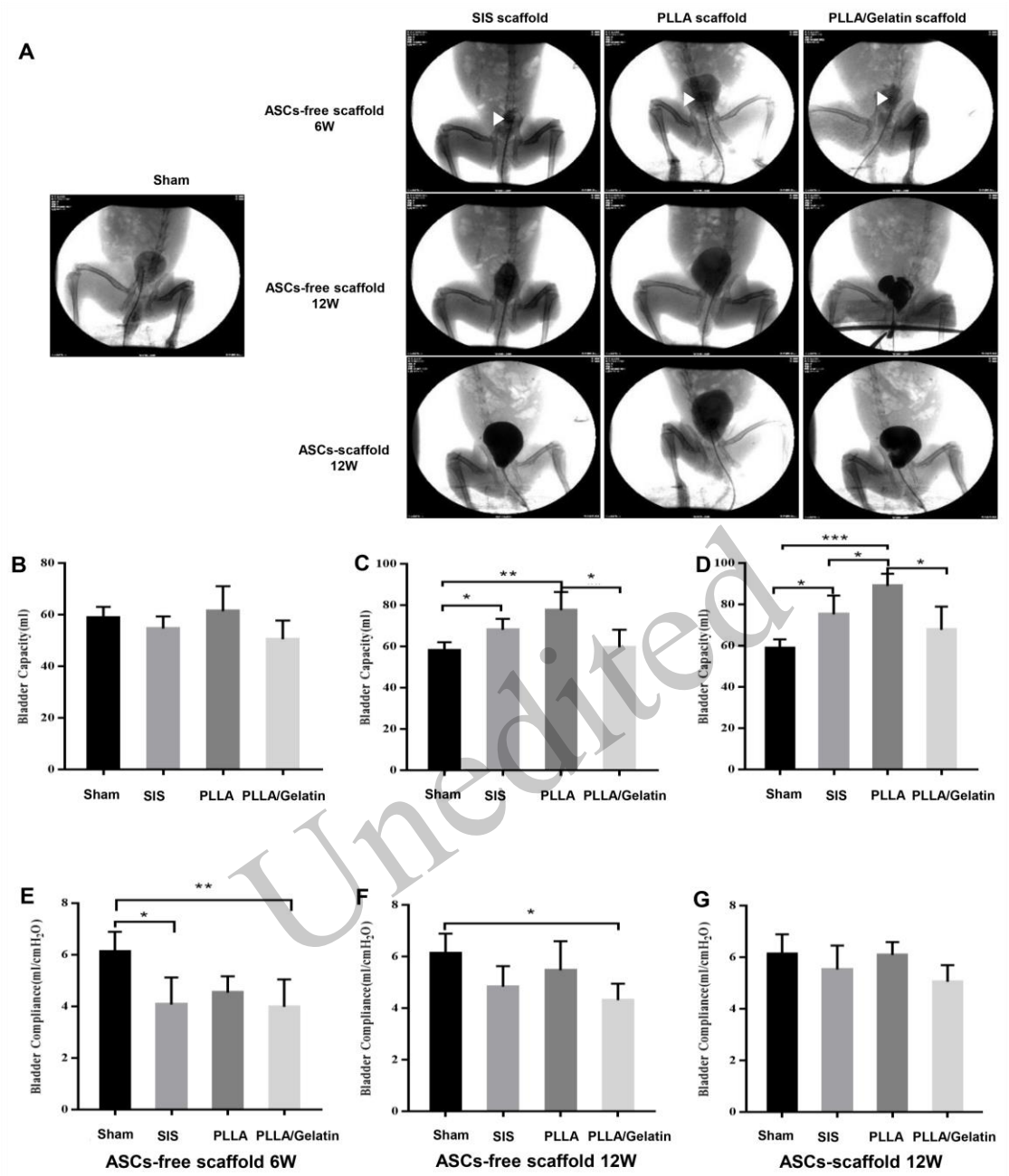

Unedited

Fig. 3 Evaluation of bladder function through cystography and urodynamics. (A) Cystography performed on different groups for evaluation of bladder morphology. 1st row: white triangle indicate bladder calculi. (B-H) The physiological function of the bladder in different groups. *P<0.05, **P<0.01, ***P<0.001.

3.4 Macroscopic evaluation

All bladder augmentation models were constructed by implanting three kinds of scaffold, with or without ASCs, into the bladder (Figure 4A). Bladder tissue from the regenerating region was harvested at scheduled time points (ASC-free scaffold: 6 weeks and 12 weeks; ASC-laden scaffolds: 12 weeks). When sampling, we first macroscopically observed the overall structure of the bladder. The implanted area of each group showed different degrees of adhesion with peripheral tissues at all time points. At 6 weeks, contracture of the bladder appeared in all ASC-free scaffold groups, but by 12 weeks, the area of bladder contracture at the graft site had

decreased significantly (Figure 4B). Scarring and shrinkage of the ASC-laden scaffolds at the regenerated site had significantly improved at 12 weeks compared with the ASC-free scaffolds. Moreover, the scarring and contracture of the ASC-PLLA group were found to be significantly superior to that of the other groups. In the study of ASC-free scaffold transplants, we observed bladder calculi only at 6 weeks in the SIS, PLLA nanofiber scaffold, and PLLA/gelatin groups, and the incidence of bladder calculi was about 40%, 20%, and 20%, respectively, in the three materials.

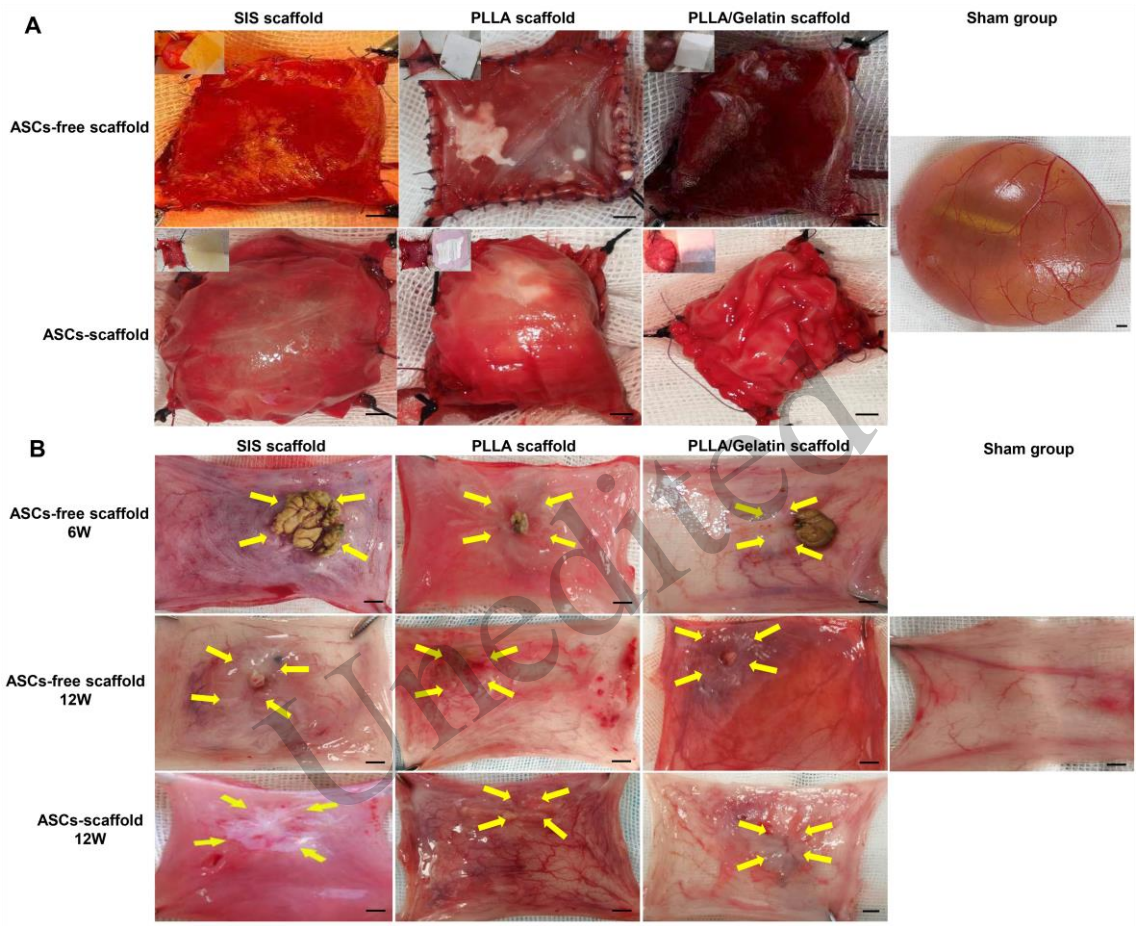

Fig. 4 Bladder reconstruction and gross evaluation. (A) Implantation of scaffolds in rabbit bladder. Scale bar = 3 mm. (B) Gross observation of urinary bladder and stones at 6 and 12 weeks after surgery in scaffolds. Scale bar = 3 mm.

3.5 Histological evaluation

H&E staining revealed that the regenerated urothelium had grown into the implanted areas from the native periphery tissues in all ASC-free scaffold groups at 6 weeks, yet the regenerated epithelium in each group was weak and incomplete compared with the native tissue epithelium (Figure 5A, B). At 12 weeks, the epithelium in the regenerated areas was multilayered in all groups but lacked the continuity, homogeneity, and mature differentiation of the natural bladder (Figure 5C). Disordered smooth muscle tissues and more fibrous tissues were detected in all groups except PLLA in the regenerated areas. In the study of ASC-laden scaffold regeneration, the regenerated epithelium in all groups except ASCs-PLLA/gelatin was similar to the native bladder epithelium (Figure 5D). Moreover, normal longitudinal and/or circular muscle band tissue regeneration was observed in all groups.

Unedited

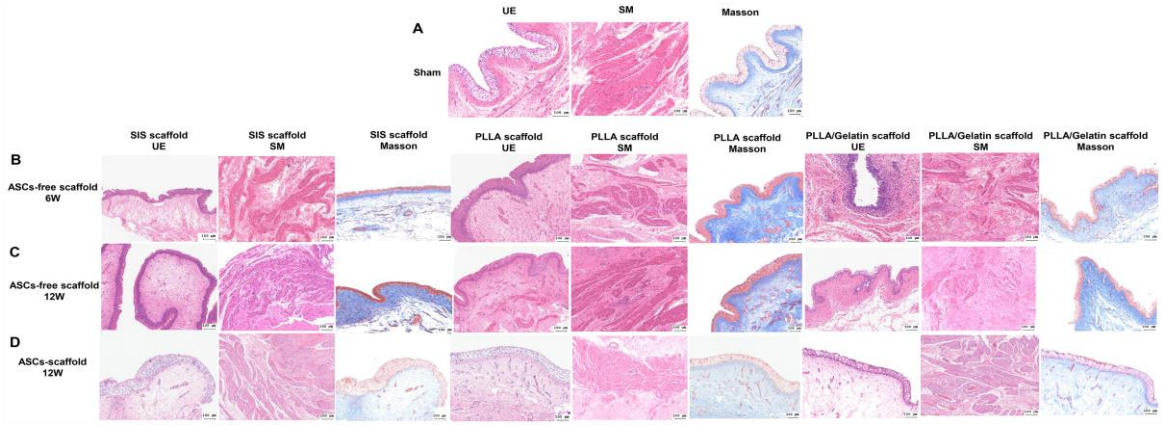

Fig. 5 Histological and morphological evaluation of regenerated bladder tissue in sham and experimental groups. (A) Hematoxylin and eosin and Masson staining indicated normal bladder tissue in the sham. (B) Regenerated bladder tissue in adipose stem cell-free scaffold at 6 weeks. (C) Regenerated bladder tissue in ASC-free scaffold at 12 weeks. (D) Regenerated bladder tissue in ASC scaffold at 12 weeks. Scale bars = 100 μm.

Bladder tissue of the regenerated area was also evaluated by IF analyses (Figure 6A). The results were consistent with H&E staining; IF staining showed that the ratios of the AE1/AE3-positive area in the three types of ASC-free scaffolds were higher at 12 weeks than at 6 weeks, but lower than that of natural bladder tissue. The urothelium morphology of the three types of ASC-laden scaffolds was similar to that of the sham group. This result was confirmed by quantitative morphometric analysis; the percentages of the AE1/AE3 area/total area in the three ASC-laden groups at 12 weeks were no different from that in the sham group (13.38 ± 1.23%, 14.46 ± 0.76, and 12.73 ± 1.93 vs. 14.06 ± 0.77%, respectively; all P> 0.05), and there were no significant differences among the three ASC-laden groups (Figure 6B). The ASC-free scaffolds had regenerated muscle fibers at 6 weeks, although they were disorganized in structure and "naive-like", indicating incomplete regeneration.

Some disordered smooth muscle-like tissues were found in the regenerated areas in the ASC-free groups at 12 weeks, but the α-SMA–positive smooth muscle tissues in all ASC-free groups were lower than those in the sham group (all P<0.05). However, muscle staining in the ASC-laden groups at 12 weeks confirmed that the ASC-PLLA group had more smooth muscle than the ASC-SIS and ASC-PLLA/gelatin groups (47.50 ± 2.16% vs. 34.70 ± 3.60% and 34.86 ± 1.97%, P<0.001, respectively), and the ratio of the α-SMA–positive area in the ASC-PLLA group was not significantly different from that in the sham group (47.50 ± 2.16% vs. 50.22 ± 1.98%, P>0.05) (Figure 6C). Similarly, the number of CD31-positive blood vessels increased continuously with time in the SIS, PLLA, and PLLA/gelatin groups without ASCs, but remained lower than that in the sham group (all P<0.05). The number of newly formed capillaries in the ASC-PLLA group was significantly greater than those of the other groups, demonstrating that the ASC-PLLA group had better neovascularization (Figure 6A, D).

Unedited

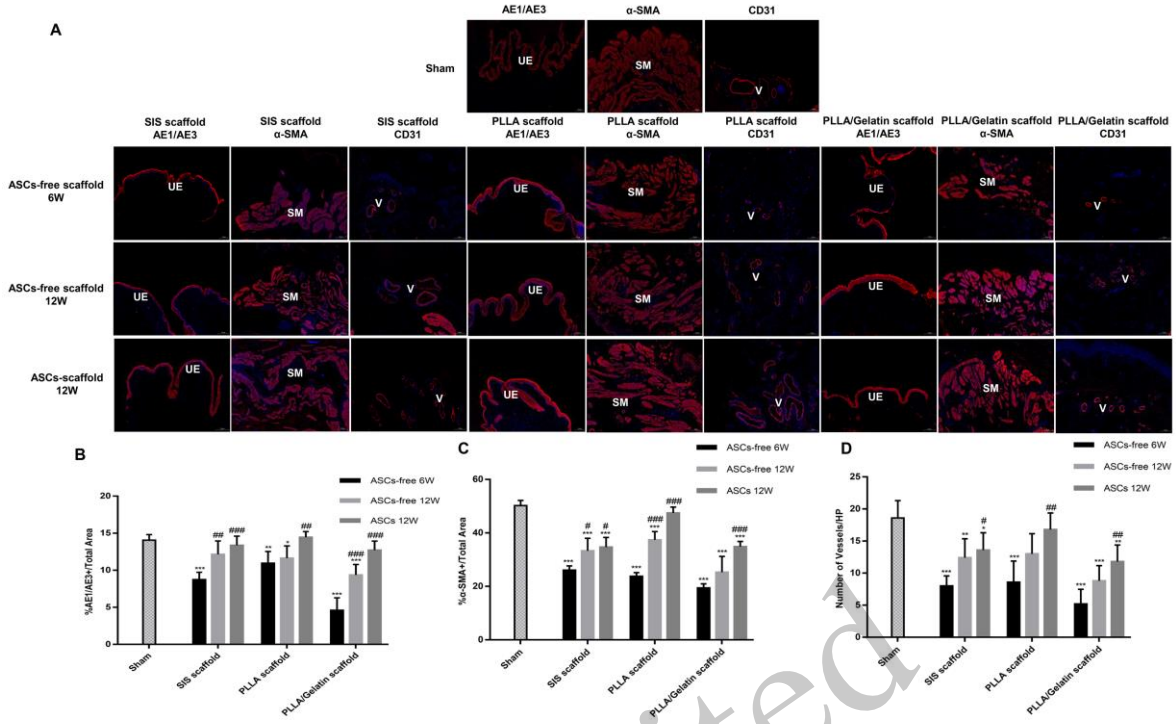

Fig. 6 Immunofluorescence staining and quantitative assessments of regenerated bladder tissue. (A) Expression of urothelial-associated markers (AE1/AE3), smooth muscle contractile markers (α-SMA), and blood vessel endothelial marker (CD31) in regenerated bladder tissue. UE: urothelium; SM: smooth muscle; V: vessels. (B, C, D) Quantitative analysis of AE1/AE3 + epithelium (B), α-SMA + smooth muscle (C), and CD31 + vessel numbers (D) in regenerated bladder tissue at 6 and 12 weeks. Scale bars = 100 μm. *P<0.05, **P<0.01, ***P<0.001 compared with sham group. #P<0.05, ##P<0.01, ###P<0.001 compared with ASC-free at 6 weeks.

Unedited

4 Discussion

A suitable barrier scaffold plays a crucial role in the tissue engineering of bladder regeneration. A variety of biomaterials used in clinical practice, such as SIS and PLLA-based biomimetic materials, have received much attention from an academic viewpoint in the field of tissue regeneration and have been shown to promote regeneration of different tissues (Colvert et al., 2002; Yang et al., 2004; Caione et al., 2006; Palminteri et al., 2007; Wu et al., 2011). However, due to the different objectives and materials of the research, a systematic evaluation of safety and effectiveness in constructing a tissue-engineered bladder is lacking. In this study, we systematically appraised the potential of PLLA-based biomimetic materials for bladder reconstruction compared them with SIS material to facilitate the selection of appropriate materials to guide future clinical research.

SEM showed that the biodegradable nonwoven PLLA and PLLA/gelatin nanofiber scaffold manufactured by electrospinning boasts open, highly interconnected pores and a unique 3D structure that resembles the ECM of the human tissue. In contrast, the structure of SIS scaffold was flat and smooth without a porous, dense surface. The pore size and porosity of regenerated materials are always two of the most important criteria to consider (Huang et al., 2016) because they promote adequate cell seeding and infiltration and increase vascular ingrowth (Joshi et al., 2013). The increased pore size and porosity of cell-free scaffolds (PLLA and PLLA/gelatin) facilitated the infiltration of abundant ASCs and the cell attachment rate was not significantly different from that of FBN-coated scaffolds. In addition, an appropriate pore size and porosity are essential for the diffusion of nutrients, metabolic waste, and gases (Baumert et al., 2007; Rnjak-Kovacina and Weiss, 2011). In another study, vascular smooth muscle cells were found parallel to synthetic microfibers 7 days after

implantation (Nivison-Smith and Weiss, 2012). Similar results were seen when vascular smooth muscle cells were implanted on synthetic material. SEM analysis demonstrated the tendency of ASCs on PLLA fibers to elongate along the long axis of the fibers. This is conducive to the spatial distribution of bladder epithelium and smooth muscle cell regeneration. Our data showed that ASC-laden scaffolds had greater bladder regeneration than other cell-free scaffolds. Moreover, the epithelium and smooth muscle formation in the models reconstructed using an ASC-PLLA scaffold was more extensive and similar to native bladder tissue than in the ASC-SIS and ASC-PLLA/gelatin groups. Of note, the regenerated bladder tissues consisting of epithelium and smooth muscle in the ASC-PLLA/gelatin group were not superior to those in the ASC-SIS and ASC-PLLA groups. That may be because the material used in the PLLA/gelatin scaffold exhibited a certain degree of hydrophilia, which led to the death of some ASCs seeded on the scaffold. Regeneration was worse than that in the ASC-PLLA group.

Excellent mechanical strength of tissue-engineered grafts is essential for bladder tissue regeneration (Deng et al., 2017). Moreover, scaffold material with favorable suture-retention and mechanical properties is also easier for surgeons to handle, and allows the graft material to be sutured. In our study, SIS, PLLA, and PLLA/gelatin biomimetic scaffolds exhibited satisfactory mechanical performance (Shi et al., 2016; Deng et al., 2017) and no animal experienced bladder rupture. In addition, prevention of urine leakage is crucial in bladder repair, and the appropriate physical and chemical properties of scaffold materials are essential to prevent leaks. The dense structure of SIS, consisting of a four-layer tissue graft, can prevent the urine traveling from the bladder to the abdominal cavity (Zhang and Liao, 2014). Note that the hydrophobic PLLA nanofiber scaffold fabricated by electrostatic spinning has hydrophobic surfaces that can serve as a barrier between fluid and the viscera and prevent fluid exudation (Shi et al., 2016). However, we observed that the PLLA/gelatin composite scaffold had some degree of hydrophilicity during implantation, which carries the risk of urine leaking into the smooth muscle layer and abdominal cavity. Moreover, transplants showed that the PLLA/gelatin scaffold was soft and not conducive to suturing. Retrograde cystography also showed an uneven overall profile. IF analysis showed inadequate regeneration of epithelium and smooth muscle in the ASC-PLLA/gelatin group, which may be due to an exudation-related inflammatory response. We evaluated the efficacy of cell-free scaffolds and cell scaffolds in bladder reconstruction. The cell-free strategy is advantageous for large-scale clinical applications because approved scaffold products can be manufactured commercially, and surrounding cells recruited by the cell-free scaffold can achieve tissue regeneration in vivo. However, implantation of cells on scaffold material is the most plausible and promising strategy to engineer tissues (Shakhssalim et al., 2017). Transplantation of cells grown on proper scaffold can accelerate tissue regeneration and prevent side effects associated with cell-free scaffolds (Atala, 2011). Native autologous cells are the ideal option, owing to the lack of immune rejection and ethical issues, as well as their consistency with the composition of bladder tissues (Wang et al., 2019).

However, mature somatic cells are not very capable of in vitro proliferation and their application is limited by long cultivation periods (Lee et al., 2018). ASCs have been widely used in bladder tissue regeneration as they are abundant and enable simple isolation and differentiation into multiple cell types (Smolar et al., 2016; Moreno-Manzano et al., 2020). In addition, previous studies have indicated that ASCs can secrete different growth factors, including vascular endothelial growth factor (VEGF) and nerve growth factor (NGF), which could promote bladder regeneration and restore bladder function (Kingham et al., 2014; Wang et al., 2017). With the development of regenerative medicine, stem cell therapy for bladder regeneration will be become a new hotspot in clinical application.

In this study, SIS, PLLA, and PLLA/gelatin membranes served as scaffolds supporting the adhesion and proliferation of ASCs. The repairing effect from the evaluation of morphology, histology, and function revealed that ASC-laden scaffolds promoted the regeneration of bladder epithelium and smooth muscle to ensure the integrity of the regenerated bladder wall. Because the ASC-PLLA biomimetic scaffold has a similar structure to the ECM and has similar dynamic and biodegradable properties, it produced a structure similar to that of native tissue in bladder augmentation.

Bladder stones are one of the most common complications seen in models with bladder augmentation.

Unedited

Rabbit urine contains high concentrations of urate, which promotes the formation of calculi (Zhao et al., 2015). Also, incompletely absorbed biomaterial fragments in the bladder lumen can serve as a nidus for calculus formation (Bury et al., 2014). In addition, some investigators have speculated that the regeneration of the intact urothelial urothelium is closely related to the inhibition of bladder stone formation (Talab et al., 2014). Our results from cystography and tissue sampling showed that bladder calculus in experimental models dissolved remarkably over time (6 to 12 weeks).

These results were also consistent with the histomorphology. Weak and incomplete regeneration of urothelium over a transplanted graft was found on the luminal side of the bladder in all model groups 6 weeks post-surgery. By 12 weeks, the experimental groups showed more mature urothelium regeneration. Appropriate porosity and large surface-area-to-volume ratios can accelerate the degradation of scaffold material (Zhong et al., 2012; Tu et al., 2013) and may also be important factors in the formation of bladder calculi. The animal models showed that the incidence of calculi in porous PLLA and PLLA/gelatin scaffolds was lower than that in the SIS group at 6 weeks, consistent with the previous conclusion that appropriate porosity and large surface-area-to-volume ratios can effectively reduce the incidence of calculi (Zhong et al., 2012; Tu et al., 2013).

Establishing a high-capacity, low-pressure allantoic capsule to preserve renal function is the ultimate goal of tissue-engineering bladder augmentation. Urodynamic evaluations are commonly used to assess changes in bladder capacity and compliance (Ajalloueian et al., 2018). Our results showed that the bladder capacity in almost all animal models increased significantly compared with the sham group at 12 weeks, but at 6 weeks there was no significant difference in bladder capacity between the reconstructed models and the sham group, and bladder compliance was generally lower than the sham. This phenomenon is consistent with the histological evaluation, in which all experimental groups showed more extensive regeneration of the epithelium, smooth muscle bundles, and vessels at the original defect sites at 12 weeks than at 6 weeks. ASCs can promote the regeneration of urothelium, smooth muscle, and blood vessels (Li et al., 2014). These results were also consistent with histological results showing that the ASC-laden models had more mature urothelium and organized smooth muscle bundles, improving bladder compliance. Notably, the ASC-PLLA group was superior to other groups in terms of bladder capacity and compliance improvement, and the histomorphological analysis revealed that the urothelium and smooth-muscle layers of the ASC-PLLA group were more like those of the sham group in the defect areas than those of the other groups.

Our study used healthy animals to construct a bladder augmentation model. A limitation was the lack of the application of the three materials in different disease backgrounds. Although comparative evaluation of the three degradable graft materials in bladder reconstruction was carried out, comparisons with other biomaterials requires further study. Future research should focus on evaluation of autologous ASC-PLLA scaffolds with long-term follow-up to ensure clinical applicability.

Unedited

5 Conclusions

The main objective of this work was to investigate the applicability of SIS, PLLA, and PLLA/gelatin nanofiber scaffolds to tissue-engineered bladder augmentation and compare their efficacy in bladder reconstruction. We confirmed that the available PLLA nanofiber scaffold had not only appropriate mechanical properties but also the appropriate pore size and porosity, which could facilitate suturing and bladder shape maintenance as well as the adhesion and proliferation of seeding ASCs. Analysis of ASC-laden scaffolds demonstrated that they promote epithelium, smooth-muscle and blood-vessel regeneration with structural and functional properties, and that the structure of the reconstructed tissue was similar to that of the native bladder. In summary, the suitability of PLLA and PLLA/gelatin nanofiber scaffolds for bladder reconstruction has been confirmed in animal models. Satisfactory results have now also been achieved in the application of ASC-PLLA scaffolds for bladder regeneration, and the results of this study provide evidence for their clinical application.

Data availability statement

The data are available from the corresponding author on reasonable request.

Acknowledgments

This work is supported by the China Rehabilitation Research Center Key Projects (CRRC Key Projects-2020-08) and Combination Cultivation Program of University of Health and Rehabilitation Sciences and China Rehabilitation Research Center (2020kfdx-006). We thank the editorial team of Home for Researchers (www.home-for-researchers.com) for the language assistance.

Author contributions

Conceptualization – Limin LIAO and Tao XU; Supervision – Limin LIAO and Liliang OUYANG; Investigation – Limin LIAO and Liliang OUYANG; Formal analysis – Xuesheng WANG, Dezhi ZHOU and Fan ZHANG; Funding acquisition – Limin LIAO and Fan ZHANG; Writing – original draft: Xuesheng WANG and Dezhi ZHOU

Compliance with ethics guidelines

Xuesheng WANG, Dezhi ZHOU, Fan ZHANG, Tao XU, Liliang OUYANG, Limin LIAO declare that they have no conflict of interest.

All procedures followed were in accordance with the ethical standards of the Capital Medical University Laboratory Animal Welfare and Ethical Committee (NO: AEEI-2021-168).

Unedited

References

Ajalloueian F, Lemon G, Hilborn J, et al., 2018. Bladder biomechanics and the use of scaffolds for regenerative medicine in the urinary bladder. *Nat Rev Urol*, 15(3):155-174. https://doi.org/10.1038/nrurol.2018.5

Atala A, 2011. Tissue engineering of human bladder. *Br Med Bull*, 97:81-104. https://doi.org/10.1093/bmb/ldr003

Baumert H, Mansouri D, Fromont G, et al., 2007. Terminal urothelium differentiation of engineered neoureter after in vivo maturation in the "omental bioreactor". *Eur Urol*, 52(5):1492-1498. https://doi.org/10.1016/j.eururo.2007.04.098

Bury MI, Fuller NJ, Meisner JW, et al., 2014. The promotion of functional urinary bladder regeneration using anti-inflammatory nanofibers. *Biomaterials*, 35(34):9311-9321. https://doi.org/10.1016/j.biomaterials.2014.07.057

Caione P, Capozza N, Zavaglia D, et al., 2006. In vivo bladder regeneration using small intestinal submucosa: Experimental study. *Pediatr Surg Int*, 22(7):593-599. https://doi.org/10.1007/s00383-006-1705-9

Chua ME, Farhat WA, Ming JM, et al., 2020. Review of clinical experience on biomaterials and tissue engineering of urinary bladder. *World J Urol*, 38(9):2081-2093. https://doi.org/10.1007/s00345-019-02833-4

Colvert JR, 3rd, Kropp BP, Cheng EY, et al., 2002. The use of small intestinal submucosa as an off-the-shelf urethral sling material for pediatric urinary incontinence. *J Urol*, 168(4 Pt 2):1872-1875; discussion 1875-1876. https://doi.org/10.1097/01.ju.0000027285.05828.e6

Deng K, Ye X, Yang Y, et al., 2016. Evaluation of efficacy and biocompatibility of a new absorbable synthetic substitute as a dural onlay graft in a large animal model. *Neurol Res*, 38(9):799-808. https://doi.org/10.1080/01616412.2016.1214418

Deng K, Yang Y, Ke Y, et al., 2017. A novel biomimetic composite substitute of plla/gelatin nanofiber membrane for dura repairing. *Neurol Res*, 39(9):819-829. https://doi.org/10.1080/01616412.2017.1348680

Derakhshan MA, Pourmand G, Ai J, et al., 2016. Electrospun plla nanofiber scaffolds for bladder smooth muscle reconstruction. *Int Urol Nephrol*, 48(7):1097-1104. https://doi.org/10.1007/s11255-016-1259-2

Huang JW, Xu YM, Li ZB, et al., 2016. Tissue performance of bladder following stretched electrospun silk fibroin matrix and bladder acellular matrix implantation in a rabbit model. *J Biomed Mater Res A*, 104(1):9-16. https://doi.org/10.1002/jbm.a.35535

Joshi VS, Lei NY, Walthers CM, et al., 2013. Macroporosity enhances vascularization of electrospun scaffolds. *J Surg Res*, 183(1):18-26. https://doi.org/10.1016/j.jss.2013.01.005

Kingham PJ, Kolar MK, Novikova LN, et al., 2014. Stimulating the neurotrophic and angiogenic properties of human adipose-derived stem cells enhances nerve repair. *Stem Cells Dev*, 23(7):741-754. https://doi.org/10.1089/scd.2013.0396

Lam Van Ba O, Aharony S, Loutochin O, et al., 2015. Bladder tissue engineering: A literature review. *Adv Drug Deliv Rev*, 82-83:31-37. https://doi.org/10.1016/j.addr.2014.11.013

Lee SW, Ryu C-M, Shin J-H, et al., 2018. The therapeutic effect of human embryonic stem cell-derived multipotent mesenchymal stem cells on chemical-induced cystitis in rats. *International Neurourology Journal*, 22(Suppl

1):S34-45. https://doi.org/10.5213/inj.1836014.007

Li H, Xu Y, Xie H, et al., 2014. Epithelial-differentiated adipose-derived stem cells seeded bladder acellular matrix grafts for urethral reconstruction: An animal model. *Tissue Eng Part A*, 20(3-4):774-784. https://doi.org/10.1089/ten.TEA.2013.0122

Moreno-Manzano V, Mellado-Lopez M, Morera-Esteve MJ, et al., 2020. Human adipose-derived mesenchymal stem cells accelerate decellularized neobladder regeneration. *Regen Biomater*, 7(2):161-169. https://doi.org/10.1093/rb/rbz049

Nivison-Smith L, Weiss AS, 2012. Alignment of human vascular smooth muscle cells on parallel electrospun synthetic elastin fibers. *J Biomed Mater Res A*, 100(1):155-161. https://doi.org/10.1002/jbm.a.33255

Palminteri E, Berdondini E, Colombo F, et al., 2007. Small intestinal submucosa (sis) graft urethroplasty: Short-term results. *Eur Urol*, 51(6):1695-1701; discussion 1701. https://doi.org/10.1016/j.eururo.2006.12.016

Pokrywczynska M, Jundzill A, Rasmus M, et al., 2018. Understanding the role of mesenchymal stem cells in urinary bladder regeneration-a preclinical study on a porcine model. *Stem Cell Res Ther*, 9(1):328. https://doi.org/10.1186/s13287-018-1070-3

Pokrywczynska M, Jundzill A, Tworkiewicz J, et al., 2021. Urinary bladder augmentation with acellular biologic scaffold—a preclinical study in a large animal model. *Journal of Biomedical Materials Research Part B: Applied Biomaterials*, 110(2):438-449. https://doi.org/10.1002/jbm.b.34920

Rnjak-Kovacina J, Weiss AS, 2011. Increasing the pore size of electrospun scaffolds. *Tissue Eng Part B Rev*, 17(5):365-372. https://doi.org/10.1089/ten.teb.2011.0235

Shakhssalim N, Soleimani M, Dehghan MM, et al., 2017. Bladder smooth muscle cells on electrospun poly(epsilon-caprolactone)/poly(l-lactic acid) scaffold promote bladder regeneration in a canine model. *Mater Sci Eng C Mater Biol Appl*, 75:877-884. https://doi.org/10.1016/j.msec.2017.02.064

Shi Z, Xu T, Yuan Y, et al., 2016. A new absorbable synthetic substitute with biomimetic design for dural tissue repair. *Artif Organs*, 40(4):403-413. https://doi.org/10.1111/aor.12568

Smolar J, Salemi S, Horst M, et al., 2016. Stem cells in functional bladder engineering. *Transfus Med Hemother*, 43(5):328-335. https://doi.org/10.1159/000447977

Talab SS, Kajbafzadeh AM, Elmi A, et al., 2014. Bladder reconstruction using scaffold-less autologous smooth muscle cell sheet engineering: Early histological outcomes for autoaugmentation cystoplasty. *BJU Int*, 114(6):937-945. https://doi.org/10.1111/bju.12685

Tian H, Bharadwaj S, Liu Y, et al., 2010. Myogenic differentiation of human bone marrow mesenchymal stem cells on a 3d nano fibrous scaffold for bladder tissue engineering. *Biomaterials*, 31(5):870-877. https://doi.org/10.1016/j.biomaterials.2009.10.001

Tu DD, Chung YG, Gil ES, et al., 2013. Bladder tissue regeneration using acellular bi-layer silk scaffolds in a large animal model of augmentation cystoplasty. *Biomaterials*, 34(34):8681-8689. https://doi.org/10.1016/j.biomaterials.2013.08.001

Wang J, Zhang Y, Cloud C, et al., 2019. Mesenchymal stem cells from chronic pancreatitis patients show comparable potency compared to cells from healthy donors. *Stem Cells Transl Med*, 8(5):418-429. https://doi.org/10.1002/sctm.18-0093

Wang Q, Xiao DD, Yan H, et al., 2017. The morphological regeneration and functional restoration of bladder defects by a novel scaffold and adipose-derived stem cells in a rat augmentation model. *Stem Cell Res Ther*, 8(1):149. https://doi.org/10.1186/s13287-017-0597-z

Wang X, Zhang F, Liao L, 2021. Current applications and future directions of bioengineering approaches for bladder augmentation and reconstruction. *Front Surg*, 8:664404. https://doi.org/10.3389/fsurg.2021.664404

Wang Y, Liao L, 2014. Histologic and functional outcomes of small intestine submucosa-regenerated bladder tissue. *BMC Urol*, 14:69. https://doi.org/10.1186/1471-2490-14-69

Wu S, Liu Y, Bharadwaj S, et al., 2011. Human urine-derived stem cells seeded in a modified 3d porous small intestinal submucosa scaffold for urethral tissue engineering. *Biomaterials*, 32(5):1317-1326. https://doi.org/10.1016/j.biomaterials.2010.10.006

Yang F, Murugan R, Ramakrishna S, et al., 2004. Fabrication of nano-structured porous plla scaffold intended for nerve tissue engineering. *Biomaterials*, 25(10):1891-1900. https://doi.org/10.1016/j.biomaterials.2003.08.062

Zhang F, Liao L, 2014. Tissue engineered cystoplasty augmentation for treatment of neurogenic bladder using small intestinal submucosa: An exploratory study. *J Urol*, 192(2):544-550. https://doi.org/10.1016/j.juro.2014.01.116

Zhang F, Liao L, 2020. Long-term follow-up of neurogenic bladder patients after bladder augmentation with small intestinal submucosa. *World J Urol*, 38(9):2279-2288. https://doi.org/10.1007/s00345-019-03008-x

Unedited

Zhang Y, Lin H-K, Frimberger D, et al., 2005. Growth of bone marrow stromal cells on small intestinal submucosa: An alternative cell source for tissue engineered bladder. *BJU International*, 96(7):1120-1125. https://doi.org/10.1111/j.1464-410X.2005.05741.x

Zhang Y, Frimberger D, Cheng EY, et al., 2006. Challenges in a larger bladder replacement with cell-seeded and unseeded small intestinal submucosa grafts in a subtotal cystectomy model. *BJU Int*, 98(5):1100-1105. https://doi.org/10.1111/j.1464-410X.2006.06447.x

Zhao Y, He Y, Guo JH, et al., 2015. Time-dependent bladder tissue regeneration using bilayer bladder acellular matrix graft-silk fibroin scaffolds in a rat bladder augmentation model. *Acta Biomater*, 23:91-102. https://doi.org/10.1016/j.actbio.2015.05.032

Zhong S, Zhang Y, Lim CT, 2012. Fabrication of large pores in electrospun nanofibrous scaffolds for cellular infiltration: A review. *Tissue Eng Part B Rev*, 18(2):77-87. https://doi.org/10.1089/ten.TEB.2011.0390

Supplementary information:

Unedited